

Density Relaxation in Time-Dependent Density Functional Theory: Combining Relaxed Density Natural Orbitals and Multireference Perturbation Theories for an Improved Description of Excited States

Enrico Ronca,^{*,†,‡} Celestino Angeli,[¶] Leonardo Belpassi,[†] Filippo De Angelis,[†] Francesco Tarantelli,^{†,‡} and Mariachiara Pastore^{*,†}

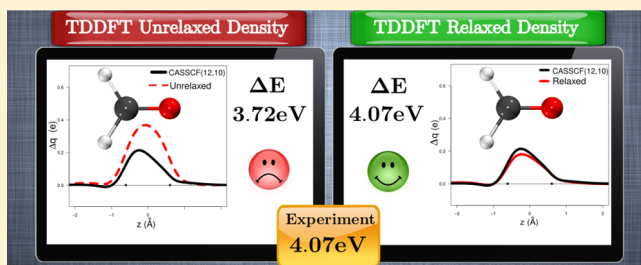
[†]Istituto CNR di Scienze e Tecnologie Molecolari, via Elce di Sotto 8, I-06123, Perugia, Italy

[‡]Dipartimento di Chimica, Biologia e Biotecnologie, Università degli Studi di Perugia, via Elce di Sotto 8, I-06123, Perugia, Italy

[¶]Dipartimento di Scienze Chimiche e Farmaceutiche, Università degli Studi di Ferrara, via Borsari 46, I-44100, Ferrara, Italy

Supporting Information

ABSTRACT: Making use of the recently developed excited state charge displacement analysis [E. Ronca et al., *J. Chem. Phys.* **140**, 054110 (2014)], suited to quantitatively characterize the charge fluxes coming along an electronic excitation, we investigate the role of the density relaxation effects in the overall description of electronically excited states of different nature, namely, valence, ionic, and charge transfer (CT), considering a large set of prototypical small and medium-sized molecular systems. By comparing the response densities provided by time-dependent density functional theory (TDDFT) and the corresponding relaxed densities obtained by applying the Z-vector postlinear-response approach [N. C. Handy and H. F. Schaefer, *J. Chem. Phys.* **81**, 5031 (1984)] with those obtained by highly correlated state-of-the-art wave function calculations, we show that the inclusion of the relaxation effects is imperative to get an accurate description of the considered excited states. We also examine what happens at the quality of the response function when an increasing amount of Hartree–Fock (HF) exchange is included in the functional, showing that the usually improved excitation energies in the case of CT states are not always the consequence of an improved description of their overall properties. Remarkably, we find that the relaxation of the response densities is always able to reproduce, independently of the extent of HF exchange in the functional, the benchmark wave function densities. Finally, we propose a novel and computationally convenient strategy, based on the use of the natural orbitals derived from the relaxed TDDFT density to build zero-order wave function for multireference perturbation theory calculations. For a significant set of different excited states, the proposed approach provided accurate excitation energies, comparable to those obtained by computationally demanding ab initio calculations.



1. INTRODUCTION

The accurate characterization of electronic excited states in molecular systems is of crucial importance for the comprehension of relevant physical and biological processes,^{1–7} as well as for improving the performance of some emerging technologies.^{8–12} Despite the great interest in the field, a correct assessment of excited-state properties remains one of the most challenging aspects for theoretical chemists.

Because of a favorable compromise between accuracy and computational cost, time-dependent density functional theory (TDDFT) dominates the scene in the study of excited states of medium- and large-sized systems.¹³ Its failure, however, in the description of charge transfer (CT),^{14–16} Rydberg,^{17–19} and double-excited states²⁰ is well-known and well-documented in the literature. The TDDFT drawback in the description of CT states is usually ascribed to the incorrect asymptotic behavior of the exchange–correlation potential (v_{xc}), resulting in a “badly underestimated”²¹ long-range charge transfer energy (approximately equal to an orbital energy difference, $\epsilon_a - \epsilon_i$). The

inclusion of an increasing percentage (>50%)^{14,16} of Hartree–Fock (HF) exchange in v_{xc} and the use of range-separated hybrid functionals^{22–28} are the most commonly employed strategies to practically overcome this inconvenience.²⁹ On the basis of this interpretation, well-established models have been also formulated to characterize different excitations according to their long-range behavior.³⁰ Despite their wide application, these strategies have the “disturbing” characteristic of describing ground and excited states with different exchange–correlation functionals,²¹ and, more importantly, these approaches fail in reproducing excitation energies of organic/inorganic molecule/metaloxide complexes, for example, dye@TiO₂^{29,31} or molecular aggregates for organic solar cells.^{11,12}

Casida et al.,³² in a detailed study performed on prototype systems, showed that the discussed TDDFT failure actually occurs only when the electron transfer process is accompanied by

Received: May 28, 2014

a sizable *density relaxation*. In this context, several approaches have been developed to account for orbital rearrangement effects, either based on improvements of the exchange-correlation functional inside the TDDFT framework³² or on a constrained self-consistent optimization of the excited states.^{33–37} Relaxation effects can be included within the TDDFT framework also using approaches that go beyond the adiabatic approximation, but usually these procedures are too computationally demanding to be widely applied.^{38–42}

Another well-established strategy developed to improve the orbital description within TDDFT and, at the same time, to overcome the double-excitation issue is the spin-flip (SF) approach.⁴³ In this case a triplet state is chosen as a reference, and the target singlets are described by spin-flipping electrons from the reference; on the generated configurations, TDDFT or more elaborated perturbation theories can then be applied to recover a larger amount of electronic correlation.^{44–48}

Outside the TDDFT scheme, several approaches are able to correctly describe CT states using either single or multireference treatments of the problem. Noteworthy examples of methods belonging to the single reference class are CIS, CIS(D),⁴⁹ NOCI,⁵⁰ CCn,⁵¹ EOM-CC,⁵² ADC,⁵³ and the Bethe–Salpeter equation.⁵⁴ Modified versions of these approaches, endowed with orbital optimization algorithms to properly account for density relaxation effects, have also been formulated.^{55–57} When more than one determinant is relevant to properly describe the system, a multireference treatment becomes necessary to account for the so-called static (near degeneracy of different electronic configurations) and dynamic correlation effects. The most-employed strategy is usually to account for the static correlation by means of a complete/restricted active space self-consistent field (CAS/RASSCF) calculation and then to recover the remaining correlation energy by configuration interaction (MRCI),^{58,59} perturbation theory (MRPT),^{60,61} or coupled cluster (MRCC) methods.⁶² Despite their accuracy, however, the high computational cost of these approaches usually does not allow their large-scale application to the description of complex systems in realistic environments.

Summarizing, if on the one hand, TDDFT is not, or at least not completely, able to account for density relaxation effects, then on the other hand, the methods developed to include orbital rearrangements, usually capable of improving the description of CT and other problematic excited states, turn out to be rather expensive in terms of computational resources. Thus, a generally accurate and computationally inexpensive theoretical strategy, to solve these drawbacks, has still to be developed.

In the present work, exploiting the excited state charge displacement (ESCD) analysis,⁶³ recently proposed by us to characterize the charge flows accompanying electronic excitations, we show the crucial role of density relaxation effects in the overall description of different kinds of excited states (valence, ionic, and CT states). In particular, considering a large set of small- and medium-sized molecular systems, which are commonly chosen as prototypes for high-level benchmark calculations, we investigate the effect of the electron density relaxation by comparing the response density directly provided by TDDFT, with a relaxed density obtained by applying the well-established Z-vector postlinear-response approach.⁶⁴ The moderate size of the investigated systems allows us also to compare the TDDFT densities with those obtained by accurate state-of-the-art wave function calculations. In the last part of the paper, we propose a novel strategy, based on merging DFT linear response and correlated wave function approaches (multi-

reference perturbation theory, MRPT), to obtain accurate excitation energies including density relaxation effects.

The paper is organized as follows. In Section 2, after a brief review of the ESCD approach, the strategy is applied to quantify the importance of the relaxation of the electron density in the description of different electronic excitations. In Section 3 the relation between the amount of nonlocal Hartree–Fock exchange, being usually increased to correct the excitation energy of CT and Rydberg states, and the quality of the associated electron density is discussed on the basis of a detailed ESCD analysis. Section 4 is instead dedicated to the description and testing of the proposed computational strategy to get accurate excitation energies exploiting a computationally cheap relaxation of the electron density within an MRPT calculation. A short summary and some concluding remarks are reported in Section 5.

2. RELAXATION EFFECTS ON THE EXCITED STATE ELECTRON DENSITY: CHARGE DISPLACEMENT ANALYSIS

The CD^{65,66} approach, as applied to electron excitations,⁶³ is based on the function Δq defined as

$$\Delta q(z) = \int_{-\infty}^z dz' \int_{-\infty}^{+\infty} \int_{-\infty}^{+\infty} \Delta \rho(x, y, z') dx, dy \quad (1)$$

Here $\Delta \rho(x, y, z)$ represents the electron density difference between the excited and ground states in exam. $\Delta q(z)$ measures, at each point along a chosen z axis, the electron charge that, upon electron excitation, is transferred from the right to the left side of the perpendicular plane through z ; a negative value thus corresponds to electron flow from left to right. In this way, the method gives a clear picture of the direction and extent of electron transfer over the whole molecular region without needing any particular model of charge decomposition.

It is important to notice, here, that linear response methods directly provide the electron density difference between the ground and the considered excited states (response function, T), which is described as a linear combination of determinants built by single excitation (de-excitation) of electrons from occupied (virtual) to virtual (occupied) ground-state orbitals. This strategy in principle neglects, or at least permits to a marginal extent, the inclusion of relaxation effects in the response function, being relaxation described by single excitations on top of single excited determinants in which the density is expanded.

Improvements to the T density difference can be obtained by resorting to the well-known Z-vector method⁶⁷ originally proposed by Handy and Schaefer.⁶⁴ This post-TDDFT approach provides, by means of a variational optimization, an additional term (Z) to the density difference matrix representing a correction associated with orbital relaxation. By adding this component to the response function one obtains the *relaxed* density difference:

$$P = T + Z \quad (2)$$

This “corrected” density by virtue of its variational nature is usually employed for the calculation of TDDFT excited-state derivative properties, which have been shown to better reproduce the experimental observables.^{68–70}

We investigated a set of systems with excited states of different nature: the first valence 1A_2 excited state of formaldehyde, the first ionic 1B_u excited state of hexatriene, and the first singlet CT state of *p*-nitroaniline (pNA). All the TDDFT calculations presented here were performed using the B3LYP exchange-

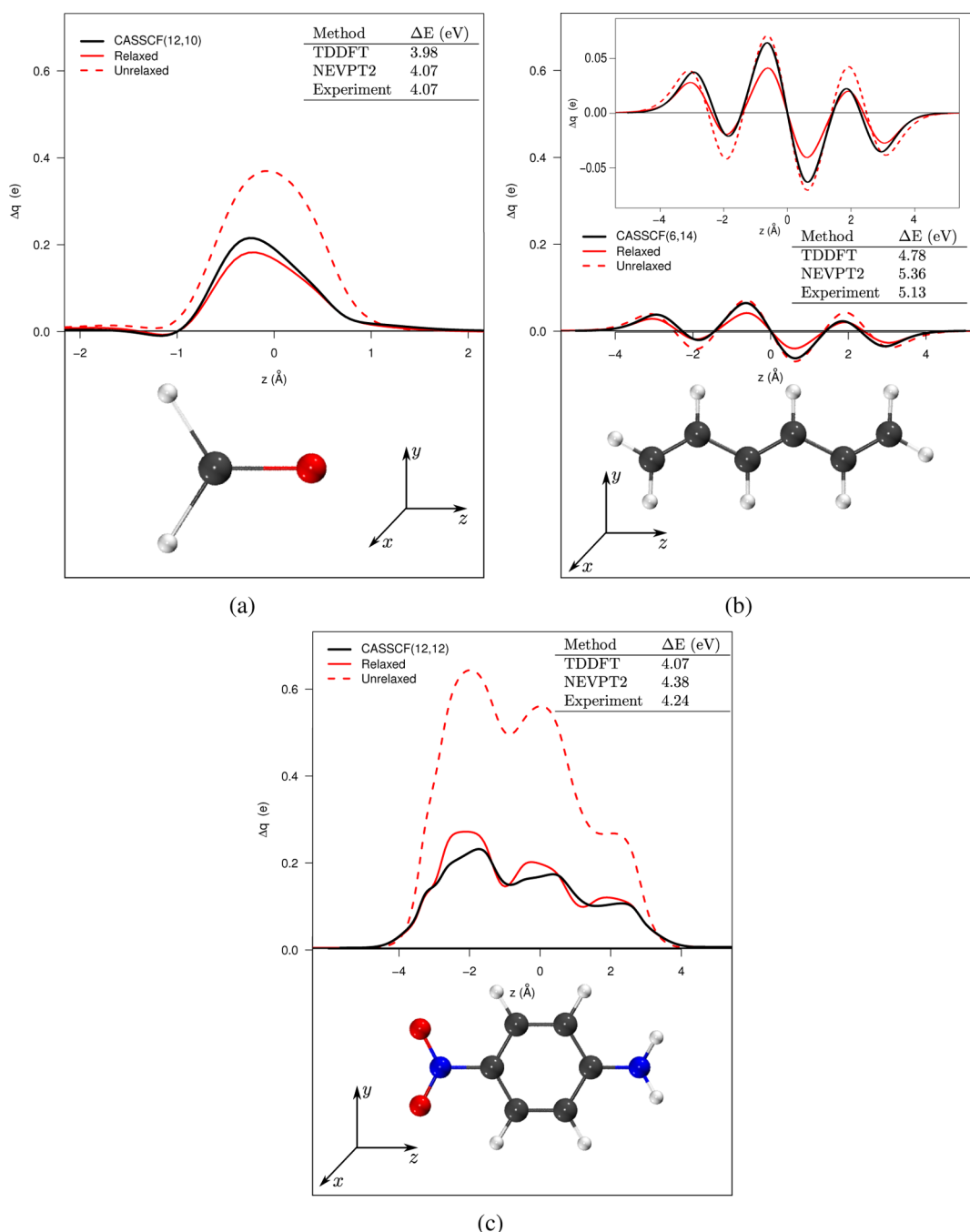


Figure 1. ESCD curves evaluated using the unrelaxed (dashed red) and relaxed (solid red) excited state electron densities in comparison with ab initio references (solid black line) evaluated at the CASSCF level for the formaldehyde 1^1A_2 (a), the hexatriene 1^1B_u (b), and the first *p*-nitroaniline (c) CT excited states. The TDDFT/B3LYP excitation energies as well as the NEVPT2 ones calculated on the corresponding reference CASSCF wave functions are also reported.

correlation functional and the 6-311G** basis set by means of the Gaussian 09 software package.⁷¹ Only in the formaldehyde case a larger basis set (aug-cc-pVQZ) was used. Complete computational details for the reported calculations are provided as Supporting Information. To benchmark the TDDFT CD functions we use accurate CASSCF densities, whose second-order corrected energies (NEVPT2)^{61,72} yield excitation energies in agreement with the corresponding experimental values (see results reported in tables within Figure 1). For these calculations the MOLPRO package was used.⁷³ ESCD analysis performed along the axis corresponding to the main charge

movements direction (z) are reported in Figure 1. The curves integrated along the perpendicular directions do not provide much additional information and are included in the Supporting Information.

In Figure 1a the ESCD curves for the first 1^1A_2 state of formaldehyde are depicted. Referring the interest reader to ref 63 for a more detailed analysis, here we just observe that this transition, in a single-particle picture, involves the promotion of one electron from a nonbonding n orbital on the oxygen atom to the π^* molecular orbital (MO) on the carbonyl group. This is reflected by the significant charge movement from the oxygen

toward the carbon atom in the ESCD curves. A small and opposite charge transfer can be also observed in the hydrogen atoms region. Figure 1a reveals that the unrelaxed TDDFT response function (dashed red line) is already qualitatively able to describe the main features of the electron density rearrangements when compared to the ab initio reference (solid black line corresponding to the CASSCF(12,10) density). In ref 63 we demonstrated this zero-order CASSCF density is in good agreement with the second-order NEVPT corrected one. (The corresponding ESCD curves are reported in Supporting Information.) The extent of the transferred charge in the TDDFT unrelaxed curve is, however, largely overestimated with respect to the reference ones: $0.37 e^-$ versus $0.21 e^-$ extracted at the maximum position in the carbonyl region. This gives also rise to small qualitative differences, particularly in the hydrogen atoms region, where the TDDFT unrelaxed curve never crosses the zero, thus completely missing the small electron transfer in the opposite direction. On the other hand, the relaxed response (solid red line) shows an overall good agreement with the ab initio reference, with an estimated transferred charge of about $0.18 e^-$; upon relaxation also the small charge flow from the hydrogen atoms toward the carbon is restored.

The accuracy of the relaxed density is further confirmed by the data reported in Table 1, where the excited-state dipole moments

Table 1. Calculated and Experimental Excited State Dipole Moments

density	μ_{ES} (D)
formaldehyde (1A_2 state)	
TDDFT/B3LYP unrelaxed	-0.22
TDDFT/B3LYP relaxed	-1.40
CASSCF(12,10)	-1.29
experimental ^a	-1.56 ± 0.07
<i>p</i> -nitroaniline (1CT state)	
TDDFT/B3LYP unrelaxed	20.81
TDDFT/B3LYP relaxed	12.40
CASSCF(12,12)	16.35
experimental ^b	13.35

^aReference 74. ^bReference 75.

evaluated using the relaxed/unrelaxed TDDFT and the ab initio reference densities are compared with the corresponding experimental values. As expected on the basis of the ESCD curves, for the formaldehyde case the ab initio reference density and the TDDFT relaxed one well reproduce the experimental value (errors never exceeding 0.3 D, that is, $\approx 20\%$ of the experimental value), whereas the unrelaxed density significantly underestimates the dipole moment (about 1.34 D less than the corresponding measured value, that is, an error larger than 80%).

Turning now our attention to the hexatriene molecule, Figure 1b shows the ESCD curves for the transition from the ground to the first singlet excited state in symmetry 1B_u . This excitation, like in the other polyenes, has mainly highest occupied molecular orbital \rightarrow lowest unoccupied molecular orbital (HOMO \rightarrow LUMO) character. Despite its one-determinant character, the ionic nature of this excited state makes its accurate description a challenge also for highly correlated and computationally expensive ab initio methods.^{50,76–80} This behavior is principally due to the presence of a consistent σ rearrangement associated with the $\pi \rightarrow \pi^*$ excitation, requiring a large amount of dynamical correlation to be properly taken into account. For this reason we choose as reference (solid black line) the density from

a large CASSCF calculation, obtained by distributing the 6 π electrons into 14 π orbitals (6,14). Application of perturbation NEVPT correction on this zero-order wave function yields rather accurate excitation energies compared to the corresponding experimental values (see Table in Figure 1b). A CASSCF density convergence evaluation as a function of the active space dimensions is reported in the Supporting Information.

The ESCD curves (Figure 1b) show an alternation of charge accumulation (positive slope) and depletion (negative slope) regions. As in the formaldehyde case, although here the relaxation effects appear to be moderate, the unrelaxed TDDFT response tends to overestimate the amount of transferred charge with respect to the ab initio reference, and again, an improved description is obtained using the relaxed density, although few discrepancies persist in the central C–C bonds, further attesting to the problematic description of this state, as discussed above. In this case the relaxation can be interpreted as the result of the σ rearrangements on the response function, which is completely neglected in the unrelaxed case. Polarization of the σ orbitals, partially compensating the positive holes produced by the excitation, tends to decrease the amount of total charge moved; this explains the CT reduction observed in the ESCD curves when the relaxation effects are included. It is extremely interesting that, as the active space increases and the second-order energy becomes closer to the experimental value (see curves and data in the Supporting Information), the difference between the relaxed B3LYP curve and the ab initio one progressively decreases. For this system no considerations about the dipole moment can be done, as, for symmetry reasons, it is zero for both the ground and the excited states.

We conclude this section by considering the electronic transition to the first singlet CT state of *p*-nitroaniline; the corresponding ESCD curves are reported in Figure 1c. Here the excitation produces a charge movement from the HOMO, localized on the ammine (NH_2) unit, toward the LUMO, principally extending over the nitro (NO_2) group. The ESCD reference curve (solid black line, evaluated at the CASSCF-(12,12) level of theory) predicts a sizable CT from the NH_2 to the nitro group, with about $0.22 e^-$ of charge reaching the oxygen atoms (evaluated at the maximum position close to the NO_2 group). In line with what previously discussed, the TDDFT unrelaxed density strongly overestimates the amount of electrons transferred to the nitro group ($0.64 e^-$). On the other side, we note the perfect qualitative and quantitative ($\sim 0.25 e^-$ transferred to the nitro group) agreement between the TDDFT relaxed ESCD curve and the ab initio reference. The accuracy of the relaxed density is further attested by the calculated excited state dipole moment (see Table 1), which almost coincides with the corresponding experimental value. Not surprisingly, considerably overestimated is the excited-state dipole moment evaluated using the unrelaxed density (about 8 D larger than the experimental one).

Summarizing, the ESCD analysis shows that the inclusion of relaxation effects is mandatory to obtain an accurate description of excited states. Although this aspect has been already investigated^{68–70} when dealing with excited-state properties (dipole moments, polarizabilities, etc.), here we quantify the effects produced by orbital relaxation via directly looking at the excited-state electron density. On the basis of these results and of the overall agreement between the benchmark ab initio curves and the TDDFT relaxed ones, we can conclude that this kind of analysis might be employed to evaluate the quality of the CASSCF wave function in MRPT calculations when large

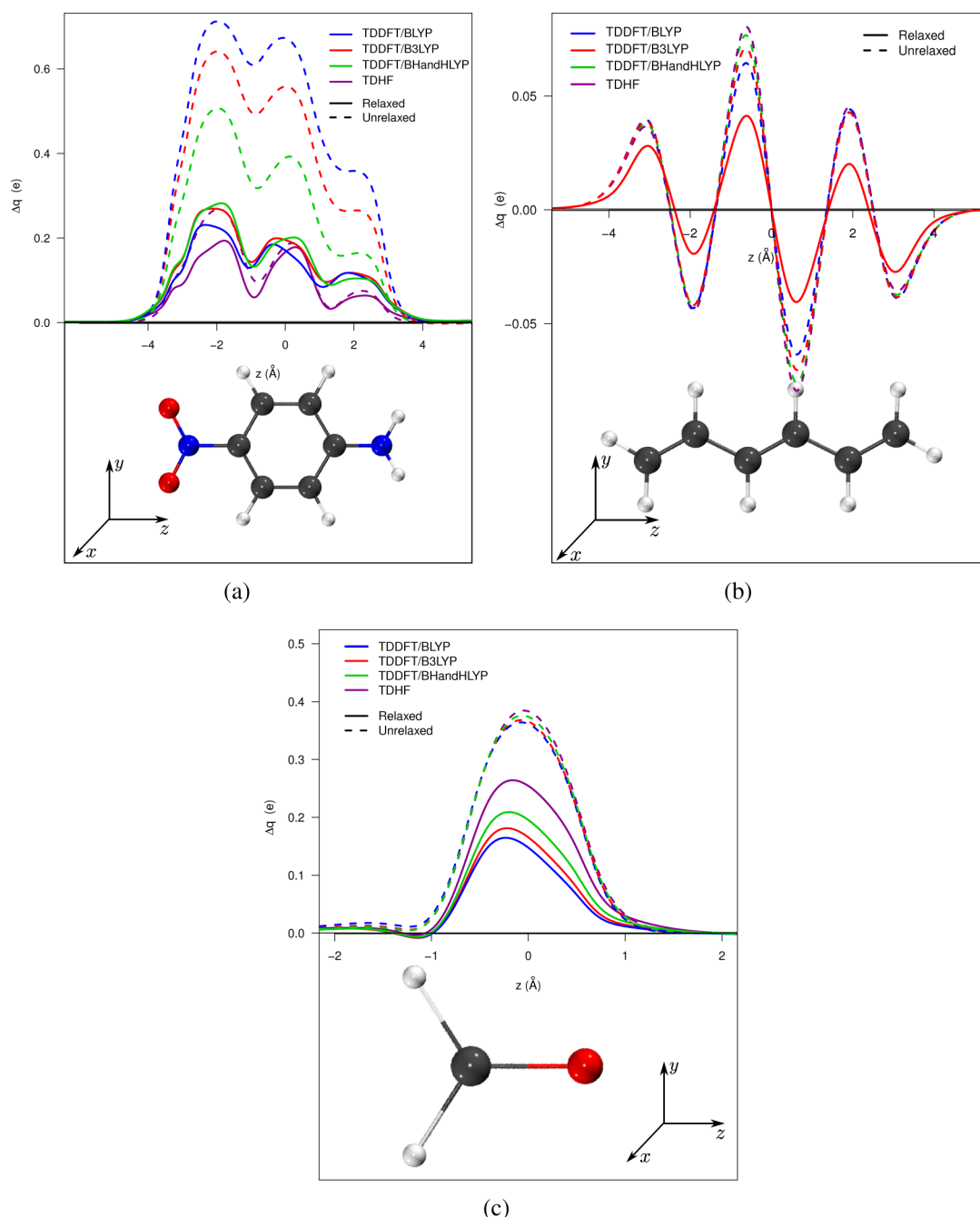


Figure 2. Effect of HF exchange percentage on the ESCD curves for excitations to the first ^1CT state of pNA (a), the $^1\text{B}_u$ state of hexatriene (b), and to the $^1\text{A}_2$ state of formaldehyde (c). Solid (dashed) lines correspond to ESCD evaluated with relaxed (unrelaxed) excited-state electron densities.

molecular sizes or “particularly difficult” excited states require a careful selection of the active space composition.

3. HARTREE–FOCK EXCHANGE EFFECTS ON THE LINEAR RESPONSE

As discussed in the Introduction, increased HF exchange percentages in the ground-state exchange–correlation functional are usually adopted to correct the TDDFT excitation energy of CT excited states. The success of this strategy is generally attributed to an improved agreement between the HOMO–LUMO gap⁸¹ and the ionization potential (IP)–electron affinity (EA) difference.¹⁶ Despite several studies that discuss the effect of the HF exchange on the excitation energy,^{14,16,22–28} very little information is present in the literature about its effect on the

response function. In this perspective, the ESCD analysis appears to be a useful tool to investigate the modifications on the electron density response produced by increasing the amount of HF exchange in the functional.

The excited states of pNA, hexatriene, and formaldehyde will be used as test cases: their ESCD curves evaluated using functionals differing for the percentage of HF exchange (BLYP 0%, B3LYP 20%, BHandHLYP 50%) as well as with the time-dependent Hartree–Fock (TDHF, 100%) are reported in Figure 2. In this plot different colors correspond to different exchange–correlation functionals (BLYP \rightarrow blue, B3LYP \rightarrow red, BHandHLYP \rightarrow green, TDHF \rightarrow purple), whereas solid and dashed lines are used for distinguishing ESCD curves evaluated with unrelaxed and relaxed densities, respectively.

As is apparent in Figure 2a, in the pNA case, the progressive increase of the HF exchange percentage significantly modifies the unrelaxed response function. In particular a systematic reduction in the amount of transferred charge, as the HF exchange increases, can be observed: BLYP \rightarrow 0.71 e⁻, B3LYP \rightarrow 0.64 e⁻, BHandHLYP \rightarrow 0.50 e⁻, TDHF \rightarrow 0.26 e⁻, extracted at the maximum in the NO₂ region. Interestingly, we notice that increasing the HF exchange percentage brings the unrelaxed density closer to the relaxed references reaching an almost perfect agreement when the TDHF approach (100% of HF exchange) is applied. An “average” estimation of the percentage error for the unrelaxed curve with respect to the relaxed reference can be obtained considering the relative differences in the CT at the positions of the three maxima. Taking as reference the B3LYP relaxed curve, we calculate for the corresponding unrelaxed one a percentage error of about 150%, which indicates an error significantly larger than the actual charge displacement (i.e., that predicted by the relaxed B3LYP and ab initio densities). As expected, the relative error is dramatically reduced going to TDHF, where a still tolerable value of about 15–20% is calculated.

On the other hand, independently of the employed functional, the relaxed response functions show an overall similarity in the whole molecular region, providing accurate quantitative information on the transferred charge. In other words, the Z-vector approach, accounting for relaxation effects, seems to properly correct (in the right different amount) the response function regardless of the quality of the starting density.

These conclusions are also corroborated by the calculated excited state dipole moments of the CT state reported in Table 2. Looking at the “unrelaxed” results, in line with the behavior of the response functions (Figure 2a), starting from a largely over-

estimated value when the BLYP functional is used, the dipole moments consistently decrease as the HF exchange percentage increases, reaching a good agreement with the experimental value in the TDHF case. As expected, dipole moments evaluated using the relaxed densities nicely compare with the measured values, showing only a small dependence on the employed functional.

Surprisingly, and contrary to what one might expect, the progressive improvement in the response function with the amount of HF exchange is not associated with systematic corrections of the excitation energy, which, as elsewhere discussed,⁸¹ increases together with the HOMO–LUMO gap (see Table 2). In particular, while TDHF shows a rather accurate unrelaxed response, it predicts a largely overestimated excitation energy (about 0.65 eV more than the experimental value). The correct excitation energy value would instead correspond to a functional with an amount of HF exchange falling in the range of 20–50%, clearly associated with an unrelaxed density response still far from the correct one (Figure 2a).

An even stronger evidence of the missing correspondence between “correct” response and accurate excitation energy is provided by both hexatriene and formaldehyde (see Figure 2b,c). In the hexatriene case, for clarity reasons, only the B3LYP relaxed ESCD curve was added to the plot; the others can be found instead in the Supporting Information. In this system, the effect produced by an increased percentage of HF exchange on the ¹B_u state unrelaxed density, even if rather small, goes in the opposite direction with respect to pNA. In particular, looking at the central region, a slight worsening in the excited-state description compared to the relaxed curve is apparent for BHandHLYP and TDHF. Notice that all the unrelaxed responses are in this case rather far from the reference one, as for the best unrelaxed curve (i.e., BLYP) we estimated an average error over the three symmetrical maxima charge-displacement points of about 70% compared to the reference. On the other hand, it is interesting to notice that, while the response density is only slightly modified (deteriorated), the excitation energy markedly improves as the HF exchange increases: the experimental value is, indeed, well-reproduced when a percentage larger than 50% is used.

Concluding with the formaldehyde case, we notice in Figure 2c that all the unrelaxed densities have the same profile: the small charge flow from the hydrogen atoms toward the carbon is completely missed, and the CT in the carbonyl region is sizeably overestimated. For instance, considering the differences between the unrelaxed and relaxed B3LYP curves, we estimated relative average errors of about 150% in the –CH₂ zone (taking the CD values at the minimum and maximum points) and 100% in the maximum along the C=O bond. As discussed in the previous section, upon relaxation the correct shape is recovered in the hydrogens region independently of the functional, whereas a larger variability can be observed in the extent of the predicted CT along the carbonyl bond, with an apparent inverse relation between the amount of nonlocal exchange and the effect produced by the relaxation procedure. Comparing Figure 1a, Figure 2c, and the second-order corrected densities in Supporting Information (Figure 4), we can conclude that the B3LYP and BHandHLYP relaxed densities show the closer agreement with the ab initio references, as also confirmed by the small error in the calculated dipole moments (see Table 2). Similarly to the pNA case, the use of the unrelaxed TDDFT densities always provides markedly inaccurate dipole moments. To further remark on the lack of a straightforward relation between the TDDFT excitation energies and the quality of the excited state density, we notice that, while the dipoles calculated

Table 2. TDDFT Excitation Energies and Excited State Dipole Moments (Calculated Using Both the Relaxed ($\mu_{\text{ES}}^{\text{rel}}$) and Unrelaxed ($\mu_{\text{ES}}^{\text{unrel}}$) Densities) Evaluated with Different Exchange-Correlation Functionals, Compared with the Corresponding Experimental Values. TDHF Data Are Also Reported

functional	ΔE (eV)	$\mu_{\text{ES}}^{\text{unrel}}$ (D)	$\mu_{\text{ES}}^{\text{rel}}$ (D)
<i>p</i> -nitroaniline (¹ CT state)			
TDDFT/BLYP	3.61	23.57	11.71
TDDFT/B3LYP	4.07	20.81	12.40
TDDFT/BH and HLYP	4.63	16.81	12.43
TDHF	4.89	11.53	10.71
exp.	4.24 ^a	13.35 ^b	
hexatriene (¹ B _u state)			
TDDFT/BLYP	4.58		
TDDFT/B3LYP	4.78		
TDDFT/BH and HLYP	5.02		
TDHF	5.24		
exp.	5.13 ^c	<i>d</i>	
formaldehyde (¹ A ₂ state)			
TDDFT/BLYP	3.82	−0.05	−1.34
TDDFT/B3LYP	3.98	−0.22	−1.40
TDDFT/BH and HLYP	4.08	−0.39	−1.40
TDHF	4.39	−0.60	−1.26
exp.	4.07 ^e	−1.56 ± 0.07 ^f	

^aReference 82. ^bReference 75. ^cReferences 83 and 84. ^dDipole moment is vanishing for symmetry reasons. ^eReference 85. ^fReference 74.

Table 3. RD-CASCI and RD-NEVPT2 Excitation Energies Compared to the Corresponding TDDFT and Experimental Values. All Excitation Energy Values Are Expressed in eV

state	TDDFT	RD-CASCI	RD-NEVPT2-SC	RD-NEVPT2-PC	reference
			butadiene		
¹ B _u	5.90	7.70	6.38	6.36	6.25 ^a
¹ A _g	7.05	7.98	7.14	6.88	6.41 ^b
			hexatriene		
¹ B _u	4.78	6.48	5.17	5.15	5.13 ^c
¹ A _g	5.79	7.59	5.50	5.16	5.21 ^d
			octatetraene		
¹ B _u	4.07	5.73	4.37	4.36	4.41 ^e
¹ A _g	4.89	5.52	4.40	4.29	3.97, ^{f,o} 4.36, ^{g,o} 4.60 ^{h,o}
			decapentaene		
¹ B _u	3.57	5.30	3.95	3.89	4.02 ⁱ
¹ A _g	4.24	5.46	3.92	3.82	3.48 ⁱ
			formaldehyde		
¹ A ₂	3.98	3.52	4.07	4.07	4.07 ^j
			<i>p</i> -nitroaniline		
2 ¹ A ₁	4.07	5.60	4.13	4.08	4.24 ^k
pyrrole					
¹ B ₂ ⁺	6.56	7.98	6.37	6.28	6.00 ^l
			ethene–tetrafluoroethene		
¹ CT (4 Å)	6.38	9.93	8.87	8.86	≥8.90, ^m 9.54 ⁿ
¹ CT (8 Å)	7.02	12.02	11.82	11.82	≥10.70, ^m 11.34 ⁿ

^aExperimental value from ref 96. ^bBest theoretical value from ref 77. ^cExperimental value from refs 83 and 84. ^dExperimental value from ref 83. ^eExperimental value from refs 97 and 98. ^fExperimental value from ref 99. ^gExperimental value from ref 88. ^hExperimental value from ref 100. ⁱExperimental value from ref 101. ^jExperimental value from ref 85. ^kExperimental value from ref 82. ^lExperimental value from ref 102. ^mExperimental value from ref 103. ⁿBest theoretical value from ref 14. ^oNote that the experimental determination of the vertical transition is controversial. See ref 88 for further details.

by B3LYP and BHandHLYP show an error of about 80%, clearly indicating a poor description of the excited state, the associated excitation energies nicely compare with the experimental value, with differences not exceeding 0.1 eV.

4. A POSSIBLE STRATEGY TO CALCULATE EXCITATION ENERGIES FROM THE RELAXED DENSITY: THE RD-MRPT APPROACH

4.1. The Idea. In the previous Section we showed that introducing Hamiltonian modifications to obtain improved excitation energies does not necessarily lead to improvements in the general description of the excited state (response function, dipole moments, etc.). But, we also saw that the inclusion of relaxation effects is usually able to recover, independently of the employed functional, the residual correction necessary to reproduce the *ab initio* response. So a question arises: Can we use the excited-state TDDFT relaxed density to calculate accurate excitation energies? Clearly, within TDDFT the calculation of the energy associated with the relaxed excited-state density is not possible, since linear response methods perturb the DFT ground-state density. Therefore, the answer must be found outside the TDDFT framework.

It has been shown (see ref 76) that in an MRPT2 calculation, only a minimal complete active space configuration interaction (CASCI) zero-order wave function (i.e., no orbital optimization) is sufficient to obtain accurate excitation energies in ethylene, if the starting orbital set properly accounts for density polarizations (dynamic σ polarization in this case), while rather poor results are obtained when the orbitals do not incorporate such effects, even if they are computed from large active-space CASSCF calculations. Applying the proposed strategy to orbitals

optimized at the RASSCF level using large active spaces, excitation energies were obtained in good agreement with the corresponding experimental data. Following this idea, it appears reasonable to consider the TDDFT relaxed densities as a good, and computationally convenient, starting point to build zero-order wave functions for subsequent CASCI/MRPT2 calculations; this should properly account for all relaxation effects. In principle, corrections able to recover the residual electronic correlation can be added to this CASCI zero-order wave function using several strategies (CASPT, NEVPT, MRCI, etc.).^{58–61} Among these approaches, here we choose the NEVPT method, which has been proven to be particularly accurate in the description of a wide range of electronic excitations (see, for instance, refs 86–88). Moreover, thanks to a recent efficient implementation, it has also been applied to the simultaneous calculation of several excited states in large-sized transition metal complexes.⁸⁹ We notice that a similar strategy, namely, the CASCI-multireference Møller–Plesset theory based on Kohn–Sham (KS) orbitals, was proposed by Nakao and co-workers and applied to the study of excited states in small molecular systems.⁹⁰ Because of the neglect of relaxation effects, however, this approach was proven to underestimate excitation energies for those excited states characterized by strong polarization effects.

Turning now to methodological aspects, in a wave function scheme one can exploit the natural orbitals (NOs) resulting from the diagonalization of the density matrix. The idea of using NOs obtained from correlated density matrices to define zero-order wave functions has been already proposed in the literature and applied to get improved CASSCF and MRCI excitation energies.^{91–93} Here the NO sets for the ground and the excited states are obtained by diagonalizing the ground state KS (GS)

and the relaxed excited state (rel-EX, defined as the sum between the relaxed response function and the ground-state density) density matrices, respectively. No additional corrections are required for the ground state considering that its density has been self-consistently optimized and consequently already includes relaxation effects. Also, the obtained NOs have always integer occupation numbers (2, 1, or 0).

Concerning the rel-EX density diagonalization, on the other hand, Kurlancheek et al.⁹⁴ demonstrated that the inclusion of the relaxation term deriving from the solution of the Z-vector equation brings the resulting electron density to be no longer N-representable. This implies that some NOs could have occupation number >2 and <0. As a matter of fact, this inconvenience does not represent an issue in our procedure, since these anomalous occupations can be observed only in the presence of basis sets close to the linear dependency. Moreover, in the CASCI wave function this problem does not occur, and the occupation numbers correctly fall between 0 and 2. At this point, it is worthwhile to point out that, in a sort of black-box fashion, the choice of the active-space dimension and composition is driven by the numbers of the NOs of the relaxed density having occupation between 0 and 2, in turn related to the nature of the important determinants resulting from the TDDFT calculation. An interesting observed property of the NOs derived from the rel-EX density is the usually limited number of the partially occupied orbitals, which permit the use of minimal active spaces. Finally, we notice that this redefinition of the occupation numbers produces only negligible variations in the electron density, thus preserving the accuracy of the relaxed description.

In the following, we shall apply this approach, hereafter termed relaxed density multireference perturbation theory (RD-MRPT), and in this case RD-NEVPT2, to the calculation of a number of different excited states, namely, valence, ionic, and CT, in a large set of small- and medium-sized molecular systems: butadiene, hexatriene, octatetraene, decapentaene, formaldehyde, pNA, pyrrole, and the ethene–tetrafluoroethene dimer.

4.2. Computational Details. The TDDFT calculations were performed at the B3LYP/6-311G** level of theory. Convergence tests with respect to the basis set dimension were carried out, and the corresponding results are reported in the Supporting Information. CASCI calculations were performed using the Molcas 6 software package.⁹⁵ Generally, a minimal two electrons–two orbitals active space (containing HOMO and LUMO) was used for the investigated systems. The only exceptions within the polyenes series are represented by the decapentaene, whose ground-state description required the use of a larger four electrons–four orbitals space (from HOMO–1 to LUMO+1), and the valence 1A_g states, for which the same four electrons–four orbitals active space was required to properly account for the double excited character of the states.⁸⁸ Another particular case is the $^1B_2^+$ excited state of pyrrole, for which a four electrons–five orbitals active space (from HOMO–1 to LUMO+2) was used. Finally, the NEVPT2 correction (both in the strongly (SC) and partially (PC) contracted form) was carried out by means of a local version of the code interfaced with Molcas 6.⁶¹

4.3. Numerical Results. The excitation energies obtained using the RD-NEVPT2 approach for all the investigated systems, compared to the corresponding TDDFT and experimental/theoretical reference data, are reported in Table 3; for the sake of completeness we also report the zero-order RD-CASCI excitation energies. A first overall look at the data in Table 3 shows an extremely good agreement between all the RD-

NEVPT2 data and the reported reference values, with differences never exceeding 0.3 eV in the RD-NEVPT2-PC case. An important remark concerns, however, the accuracy of the 1A_g states of polyenes, for which we observe appreciable differences (in the range of 0.1–0.3 eV) between the SC and PC results, probably coming from the TDDFT electron density, which does not account for the double excited character of the transition. In particular, sizeably overestimated excitation energies (~ 0.47 eV and ~ 0.34 eV) are obtained in the case of the 1A_g excited state of butadiene and decapentaene, respectively. The comparison with the experimental values is, however, not straightforward considering that, for these dipole-forbidden 1A_g excited states, a firm experimental assignment is not available in the literature. In particular, for butadiene there is no experimental reference, and it is common practice to compare the calculated values with the “accepted” best theoretical estimation.⁷⁷ While for hexatriene and decapentaene, the two-photon absorption results are not questioned, for octatetraene the assignment is still controversial, as shown by the three reference values listed in Table 3. Also, high-level theoretical methods generally tend to overestimate these excitation energies with respect to the accepted references. For the butadiene molecule, for instance, a large variability can be found in the literature: EOM-CCSD $\rightarrow 7.23$ eV,¹⁰⁴ EOM-CCSD(T) $\rightarrow 6.76$ eV,¹⁰⁴ CC2 $\rightarrow 7.04$ eV,¹⁰⁵ SAC–CI $\rightarrow 7.05$ eV,¹⁰⁶ MR-CISD $\rightarrow 6.78$ eV.¹⁰⁷ A detailed discussion on the assignment of the ionic (1B_u) and valence (1A_g) states of polyenes is out of our scope here, where we focus instead on the general capability of our approach in describing the correct energetical order of the two states along the series. To do this we refer either to the experimental values, where available, or to the accepted best theoretical estimations. Starting from butadiene, where the 1A_g state is higher in energy than the 1B_u state, experiments indicate that the former tends to be progressively more stabilized than the latter going toward the decapentaene; their energy inversion occurs for octatetraene. The experimental trend is shown by the black lines reported in Figure 3. As is apparent, the

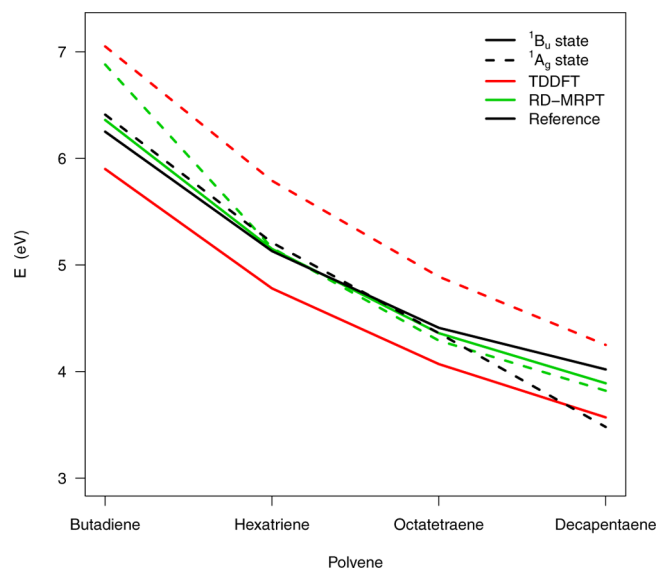


Figure 3. Excitation energy trend along the polyenes series for the 1B_u (solid) and 1A_g (dashed) excited states. Red lines refer to energy value evaluated at the TDDFT level, the green ones refer to the RD-NEVPT-PC results, and the black lines correspond to the reference values. For octatetraene the intermediate experimental value (4.36 eV) was used as reference.

RD-NEVPT2-PC results (green lines) well reproduce the expected trend providing accurate results, in particular for the 1B_u excited states. On the other hand, TDDFT (red lines) predicts, as expected, a wrong energy ordering of the two singlet excited states, with the 1A_g state lying always well-above the ionic one.

As we pointed out previously, the advantage of using the RD-NEVPT2 approach also relies in the minimal, or extremely reduced, active space dimensions required in the CASCI diagonalization step. Conventional CASSCF/MRPT calculations, instead, usually require larger spaces, including more virtual orbitals than those directly involved in the excitation to allow for orbital relaxation to a certain extent.⁸⁸ One can, indeed, observe (see Table 4) that RD-NEVPT2 is able to provide more

Table 4. CASSCF/NEVPT2 Excitation Energies Calculated with the Same Minimal Active Spaces Used in the RD-NEVPT2 Approach for the Excited States of the First Three Polyenes

state	CASSCF, eV	NEVPT2-SC, eV	NEVPT2-PC, eV
butadiene			
1B_u	7.54	6.75	6.73
1A_g	6.76	6.88	6.90
hexatriene			
1B_u	6.66	5.57	5.56
1A_g	6.47	5.78	5.75
octatetraene			
1B_u	5.73	4.57	4.56
1A_g	5.84	4.90	4.85

accurate results than those obtained by a NEVPT2 treatment starting from CASSCF wave functions calculated using the same minimal active spaces. In particular the standard multireference approach, because of a rather poor description of the zero-order electron density when small active spaces are used (see Section 2), significantly overestimates the excitation energy of both the electronic transitions and completely misses the correct energy ordering along the polyenes series. Comparable accuracy (i.e., 5.36 eV for the 1B_u state of hexatriene) can be, instead, obtained by a standard NEVPT2 calculation using a large active space (6,14), whose CASSCF ESCD curve (in Figure 1b) resulted in close agreement with the TDDFT relaxed one.

Moving on to the CT transition in the prototypical ethene–tetrafluoroethene complex, the values reported in Table 3 clearly show that the wrong radial dependence of exchange-correlation potential, yielding to strongly underestimated B3LYP excitation energies, does not affect the accuracy of the RD-NEVPT2 results. As is apparent, the method is able to recover the error of 3–4 eV found in TDDFT, bringing the excitation energies close to the expected reference values. Notice that the accuracy in the description is maintained when the distance between the two monomers increases.

The last point that deserves further discussion is the use of the unrelaxed TDDFT excited-state density (UD-NEVPT2) instead of the relaxed one. The results obtained for a representative set of systems (the first three polyenes and formaldehyde) are reported in Table 5. Comparing these data with those reported in Table 3, it definitely appears that for the 1B_u states of polyenes and in the formaldehyde case, where the inclusion of relaxation effects is essential (see Section 2), the use of the unrelaxed density leads to results significantly different from those obtained with the relaxed one and, hence, far from the corresponding experimental

Table 5. Excitation Energies Evaluated Using Unrelaxed Excited State Densities (UD-NEVPT)

state	UD-CASCI, eV	UD-NEVPT2-SC, eV	UD-NEVPT2-PC, eV
butadiene			
1B_u	8.20	5.88	5.81
1A_g	8.00	7.16	6.91
hexatriene			
1B_u	6.96	4.67	4.64
1A_g	7.66	5.52	5.17
octatetraene			
1B_u	6.13	3.94	3.91
1A_g	5.55	4.41	4.31
formaldehyde			
1A_2	4.62	3.72	3.72

values. On the other hand for the 1A_g states, generally characterized by small relaxation effects (see the ESCD curves for the hexatriene case in the Supporting Information), the unrelaxed TDDFT density is already able to provide reliable results. Indeed, for these excited states the large error observed at the TDDFT level of theory reasonably arises from the significant double-excited character, in part recovered in the RD-CASCI step.

5. CONCLUSIONS

Making use of the recently developed ESCD analysis,⁶³ we investigated the role of the density relaxation effects in the description of electronically excited states of different nature (valence, ionic, CT). By comparing both relaxed and unrelaxed TDDFT responses with benchmark CASSCF densities, we have shown that the inclusion of relaxation effects is essential to get an accurate description of the excited state properties and therefore of a quantitative estimate of the charge transferred during the excitation. We have also investigated the effects that the inclusion of an increasing amount of HF exchange in the functional (the commonly employed strategy to improve the excitation energies of CT states within the TDDFT framework) has on the quality of the corresponding response function. Remarkably, we demonstrated that the improved excitation energy is not necessarily associated with an improved description of the excited-state properties (dipole moments, extent and direction of the charge flows accompanying the electron excitation), which is, instead, always achieved, independently of the employed functional, when density relaxation is allowed. Inspired by the idea⁷⁶ that if one is able to define a good set of molecular orbitals, (already accounting for major polarization effects) the dynamic electron correlation can be more easily recovered, we propose a simple strategy to avoid large MCSCF step in multireference approaches. In particular, we replace the CASSCF optimization step in NEVPT2 calculations by using a CASCI wave function built on the ground and excited state natural orbitals obtained by diagonalizing the KS and relaxed TDDFT densities, respectively. Remarkably, for a significant set of different excited states, we have shown that the good quality of the zero-order densities allowed for the use of minimal active spaces to obtain excitation energies comparable to those provided by large CASSCF/NEVPT2 calculations.

Along with accuracy and wide applicability, a remarkable characteristic of the proposed approach is the complete elimination of the long-range issues of TDDFT, usually affecting the standard exchange-correlation functionals. From a wave function perspective, moreover, circumventing the onerous

CAS/RASSCF orbital optimization step in a MRPT calculation leads to a significant reduction in the computational cost, paving the way, possibly exploiting resolution of identity (RI) techniques,¹⁰⁸ for the accurate description of the excited states of larger systems of high applicative interest.^{109–111}

■ ASSOCIATED CONTENT

● Supporting Information

Additional computational details and several tests on ESCD curves. This material is available free of charge via the Internet at <http://pubs.acs.org/>.

■ AUTHOR INFORMATION

Corresponding Authors

*E-mail: enrico@thch.unipg.it. (E.R.)

*E-mail: chiara@thch.unipg.it. (M.P.)

Notes

The authors declare no competing financial interest.

■ ACKNOWLEDGMENTS

We thank MIUR-PRIN 2010-2011 Project No. 20104XET32 “DSSCX” for financial support.

■ REFERENCES

- (1) Bucher, D. B.; Pilles, B. M.; Carell, T.; Zinth, W. *Proc. Natl. Acad. Sci. U.S.A.* **2014**, *111*, 4369–4374.
- (2) Santoro, F.; Barone, V.; Improbato, R. *Proc. Natl. Acad. Sci. U.S.A.* **2007**, *104*, 9931–9936.
- (3) Kawai, K.; Kodera, H.; Osakada, Y.; Majima, T. *Nat. Chem.* **2009**, *1*, 156–159.
- (4) Goldsmith, R. H.; Sinks, L. E.; Kelley, R. F.; Betzen, L. J.; Liu, W.; Weiss, E. A.; Ratner, M. A.; Wasielewski, M. R. *Proc. Natl. Acad. Sci. U.S.A.* **2005**, *102*, 3540–3545.
- (5) Gray, H. B.; Winkler, J. R. *Proc. Natl. Acad. Sci. U.S.A.* **2005**, *102*, 3534–3539.
- (6) Megiatto, J. D.; Antoniuk-Pablant, A.; Sherman, B. D.; Kodis, G.; Gervaldio, M.; Moore, T. A.; Moore, A. L.; Gust, D. *Proc. Natl. Acad. Sci. U.S.A.* **2012**, *109*, 15578–15583.
- (7) Kelley, S. O.; Barton, J. K. *Science* **1999**, *283*, 375–381.
- (8) O'Regan, B.; Grätzel, M. *Nature* **1991**, *353*, 737.
- (9) Lee, M. M.; Teuscher, J.; Miyasaka, T.; Murakami, T. N.; Snaith, H. *J. Science* **2012**, *338*, 643–647.
- (10) Nocera, D. G. *Acc. Chem. Res.* **2012**, *45*, 767–776.
- (11) He, Z.; Zhong, C.; Su, S.; Miao, X.; Wu, H.; Cao, Y. *Nat. Photonics* **2012**, *6*, 591–595.
- (12) Li, G.; Zhu, R.; Yang, Y. *Nat. Photonics* **2012**, *6*, 153–161.
- (13) Runge, E.; Gross, E. K. U. *Phys. Rev. Lett.* **1984**, *52*, 997–1000.
- (14) Dreuw, A.; Weisman, J. L.; Head-Gordon, M. *J. Chem. Phys.* **2003**, *119*, 2943–2946.
- (15) Dreuw, A.; Head-Gordon, M. *J. Am. Chem. Soc.* **2004**, *126*, 4007–4016.
- (16) Dreuw, A.; Head-Gordon, M. *Chem. Rev.* **2005**, *105*, 4009–4037.
- (17) Casida, M. E.; Jamorski, C.; Casida, K. C.; Salahub, D. R. *J. Chem. Phys.* **1998**, *108*, 4439–4449.
- (18) Wasserman, A.; Maitra, N. T.; Burke, K. *Phys. Rev. Lett.* **2003**, *91*, 263001.
- (19) Hirata, S.; Zhan, C.-G.; Apra, E.; Windus, T. L.; Dixon, D. A. *J. Phys. Chem. A* **2003**, *107*, 10154–10158.
- (20) Mikhailov, I. A.; Tafur, S.; Masunov, A. E. *Phys. Rev. A* **2008**, *77*, 012510.
- (21) Casida, M.; Huix-Rotlant, M. *Annu. Rev. Phys. Chem.* **2012**, *63*, 287–323.
- (22) Yanai, T.; Tew, D. P.; Handy, N. C. *Chem. Phys. Lett.* **2004**, *393*, 51–57.
- (23) Vydrov, O. A.; Scuseria, G. E. *J. Chem. Phys.* **2006**, *125*, 234109.
- (24) Rohrdanz, M. A.; Martins, K. M.; Herbert, J. M. *J. Chem. Phys.* **2009**, *130*, 054112.
- (25) Baer, R.; Livshits, E.; Salzner, U. *Annu. Rev. Phys. Chem.* **2010**, *61*, 85–109.
- (26) Stein, T.; Kronik, L.; Baer, R. *J. Am. Chem. Soc.* **2009**, *131*, 2818–2820.
- (27) Fromager, E.; Jensen, H. J. A. *Phys. Rev. A* **2008**, *78*, 022504.
- (28) Fromager, E.; Knecht, S.; Jensen, H. J. A. *J. Chem. Phys.* **2013**, *138*, 084101.
- (29) Pastore, M.; Mosconi, E.; De Angelis, F.; Grätzel, M. *J. Phys. Chem. C* **2010**, *114*, 7205–7212.
- (30) Peach, M. J. G.; Benfield, P.; Helgaker, T.; Tozer, D. J. *J. Chem. Phys.* **2008**, *128*, 044118.
- (31) Pastore, M.; Selloni, A.; Fantacci, S.; Angelis, F. Electronic and Optical Properties of Dye-Sensitized TiO₂ Interfaces. In *Topics in Current Chemistry*; Springer: Berlin, Heidelberg, 2014; pp 1–45.
- (32) Casida, M. E.; Gutierrez, F.; Guan, J.; Gadea, F.-X.; Salahub, D.; Daudey, J.-P. *J. Chem. Phys.* **2000**, *113*, 7062–7071.
- (33) Ziegler, T.; Seth, M.; Krykunov, M.; Autschbach, J.; Wang, F. *J. Chem. Phys.* **2009**, *130*, 154102.
- (34) Ziegler, T.; Krykunov, M.; Cullen, J. J. *Chem. Theory Comput.* **2011**, *7*, 2485–2491.
- (35) Ziegler, T.; Krykunov, M.; Cullen, J. J. *Chem. Phys.* **2012**, *136*, 124107.
- (36) Krykunov, M.; Seth, M.; Ziegler, T. *J. Chem. Phys.* **2014**, *140*, 18A502.
- (37) Evangelista, F. A.; Shushkov, P.; Tully, J. C. *J. Phys. Chem. A* **2013**, *117*, 7378–7392.
- (38) Gimón, T.; Ipatov, A.; Heßelmann, A.; Görling, A. *J. Chem. Theory Comput.* **2009**, *5*, 781–785.
- (39) Heßelmann, A.; Ipatov, A.; Görling, A. *Phys. Rev. A* **2009**, *80*, 012507.
- (40) Görling, A. *Int. J. Quantum Chem.* **1998**, *69*, 265–277.
- (41) Ullrich, C. A.; Grossmann, U. J.; Gross, E. K. U. *Phys. Rev. Lett.* **1995**, *74*, 872–875.
- (42) Hirata, S.; Ivanov, S.; Grabowski, I.; Bartlett, R. J. *J. Chem. Phys.* **2002**, *116*, 6468–6481.
- (43) Shao, Y.; Head-Gordon, M.; Krylov, A. I. *J. Chem. Phys.* **2003**, *118*, 4807–4818.
- (44) Levchenko, S. V.; Krylov, A. I. *J. Chem. Phys.* **2004**, *120*, 175–185.
- (45) Sears, J. S.; Sherrill, C. D.; Krylov, A. I. *J. Chem. Phys.* **2003**, *118*, 9084–9094.
- (46) Casanova, D.; Head-Gordon, M. *J. Chem. Phys.* **2008**, *129*, 064104.
- (47) Casanova, D.; Head-Gordon, M. *Phys. Chem. Chem. Phys.* **2009**, *11*, 9779–9790.
- (48) Zimmerman, P. M.; Musgrave, C. B.; Head-Gordon, M. *Acc. Chem. Res.* **2013**, *46*, 1339–1347.
- (49) Head-Gordon, M.; Rico, R. R. J.; Oumi, M.; Lee, T. T. *J. Chem. Phys. Lett.* **1994**, *219*, 21–29.
- (50) Sundstrom, E. J.; Head-Gordon, M. *J. Chem. Phys.* **2014**, *140*, 114103.
- (51) Christiansen, O.; Koch, H.; Jorgensen, P. *Chem. Phys. Lett.* **1995**, *243*, 409–418.
- (52) Stanton, J. F.; Bartlett, R. J. *J. Chem. Phys.* **1993**, *98*, 7029–7039.
- (53) Schirmer, J. *Phys. Rev. A* **1982**, *26*, 2395–2416.
- (54) Onida, G.; Reining, L.; Rubio, A. *Rev. Mod. Phys.* **2002**, *74*, 601–659.
- (55) Krylov, A. I.; Sherrill, C. D.; Head-Gordon, M. *J. Chem. Phys.* **2000**, *113*, 6509–6527.
- (56) Liu, X.; Subotnik, J. E. *J. Chem. Theory Comput.* **2014**, *10*, 1004–1020.
- (57) Liu, X.; Ou, Q.; Alguire, E.; Subotnik, J. E. *J. Chem. Phys.* **2013**, *138*, 221105.
- (58) Werner, H.; Knowles, P. J. *J. Chem. Phys.* **1988**, *89*, 5803–5814.
- (59) Angeli, C.; Cimiraglia, R.; Pastore, M. *Mol. Phys.* **2012**, *110*, 2963–2968.
- (60) Andersson, K.; Malmqvist, P. A.; Roos, B. O.; Sadlej, A. J.; Wolinski, K. *J. Phys. Chem.* **1990**, *94*, 5483–5488.

- (61) Angeli, C.; Cimiraglia, R.; Evangelisti, S.; Leininger, T.; Malrieu, J.-P. *J. Chem. Phys.* **2001**, *114*, 10252–10264.
- (62) Laidig, W. D.; Bartlett, R. J. *Chem. Phys. Lett.* **1984**, *104*, 424–430.
- (63) Ronca, E.; Pastore, M.; Belpassi, L.; De Angelis, F.; Angeli, C.; Cimiraglia, R.; Tarantelli, F. *J. Chem. Phys.* **2014**, *140*, 054110.
- (64) Handy, N. C.; Schaefer, H. F. J. *Chem. Phys.* **1984**, *81*, 5031–5033.
- (65) Belpassi, L.; Infante, I.; Tarantelli, F.; Visscher, L. *J. Am. Chem. Soc.* **2008**, *130*, 1048–1060.
- (66) Cappelletti, D.; Ronca, E.; Belpassi, L.; Tarantelli, F.; Pirani, F. *Acc. Chem. Res.* **2012**, *45*, 1571–1580.
- (67) Furche, F.; Ahlrichs, R. *J. Chem. Phys.* **2002**, *117*, 7433–7447.
- (68) Wiberg, K. B.; Hadad, C. M.; LePage, T. J.; Breneman, C. M.; Frisch, M. J. *J. Phys. Chem.* **1992**, *96*, 671–679.
- (69) Foresman, J. B.; Head-Gordon, M.; Pople, J. A.; Frisch, M. J. *J. Phys. Chem.* **1992**, *96*, 135–149.
- (70) Cammi, R.; Mennucci, B.; Tomasi, J. *J. Phys. Chem. A* **1999**, *103*, 9100–9108.
- (71) Frisch, M. J.; Trucks, G. W.; Schlegel, H. B.; Scuseria, G. E.; Robb, M. A.; Cheeseman, J. R.; Scalmani, G.; Barone, V.; Mennucci, B.; Petersson, G. A.; Nakatsuji, H.; Caricato, M.; Li, X.; Hratchian, H. P.; Izmaylov, A. F.; Bloino, J.; Zheng, G.; Sonnenberg, J. L.; Hada, M.; Ehara, M.; Toyota, K.; Fukuda, R.; Hasegawa, J.; Ishida, M.; Nakajima, T.; Honda, Y.; Kitao, O.; Nakai, H.; Vreven, T.; Montgomery, J. A., Jr.; Peralta, J. E.; Ogliaro, F.; Bearpark, M.; Heyd, J. J.; Brothers, E.; Kudin, K. N.; Staroverov, V. N.; Kobayashi, R.; Normand, J.; Raghavachari, K.; Rendell, A.; Burant, J. C.; Iyengar, S. S.; Tomasi, J.; Cossi, M.; Rega, N.; Millam, J. M.; Klene, M.; Knox, J. E.; Cross, J. B.; Bakken, V.; Adamo, C.; Jaramillo, J.; Gomperts, R.; Stratmann, R. E.; Yazyev, O.; Austin, A. J.; Cammi, R.; Pomelli, C.; Ochterski, J. W.; Martin, R. L.; Morokuma, K.; Zakrzewski, V. G.; Voth, G. A.; Salvador, P.; Dannenberg, J. J.; Dapprich, S.; Daniels, A. D.; Farkas, Ö.; Foresman, J. B.; Ortiz, J. V.; Cioslowski, J.; Fox, D. J. *Gaussian 09*, Revision C.01; Gaussian, Inc.: Wallingford, CT, 2009.
- (72) Angeli, C.; Pastore, M.; Cimiraglia, R. *Theor. Chem. Acc.* **2007**, *117*, 743–754.
- (73) Werner, H.-J.; Knowles, P. J.; Knizia, G.; Manby, F. R.; Schütz, M.; Celani, P.; Korona, T.; Lindh, R.; Mitrushenkov, A.; Rauhut, G.; Shamasundar, K. R.; Adler, T. B.; Amos, R. D.; Bernhardsson, A.; Berning, A.; Cooper, D. L.; Deegan, M. J. O.; Dobbyn, A. J.; Eckert, F.; Goll, E.; Hampel, C.; Hesselmann, A.; Hetzer, G.; Hrenar, T.; Jansen, G.; Köppl, C.; Liu, Y.; Lloyd, A. W.; Mata, R. A.; May, A. J.; McNicholas, S. J.; Meyer, W.; Mura, M. E.; Nicklass, A.; O'Neill, D. P.; Palmieri, P.; Peng, D.; Pflüger, K.; Pitzer, R.; Reiher, M.; Shiozaki, T.; Stoll, H.; Stone, A. J.; Tarroni, R.; Thorsteinsson, T.; Wang, M. *MOLPRO*, version 2010.1, a package of ab initio programs. 2010. <http://www.molpro.net> (accessed March 23, 2014).
- (74) Freeman, D. E.; Klemperer, W. J. *Chem. Phys.* **1966**, *45*, 52–57.
- (75) Smith, B. H.; Buonaugurio, A.; Chen, J.; Collins, E.; Bowen, K. H.; Compton, R. N.; Sommerfeld, T. *J. Chem. Phys.* **2013**, *138*, 234304.
- (76) Angeli, C. *J. Comput. Chem.* **2009**, *30*, 1319–1333.
- (77) Watson, M. A.; Chan, G. K.-L. *J. Chem. Theory Comput.* **2012**, *8*, 4013–4018.
- (78) Serrano-Andrés, L.; Merchán, M.; Nebot-Gil, I.; Lindh, R.; Roos, B. O. *J. Chem. Phys.* **1993**, *98*, 3151–3162.
- (79) Wanko, M.; Garavelli, M.; Bernardi, F.; Niehaus, T. A.; Frauenheim, T.; Elstner, M. *J. Chem. Phys.* **2004**, *120*, 1674–1692.
- (80) Nakayama, K.; Nakano, H.; Hirao, K. *Int. J. Quantum Chem.* **1998**, *66*, 157–175.
- (81) Pastore, M.; Fantacci, S.; De Angelis, F. *J. Phys. Chem. C* **2013**, *117*, 3685–3700.
- (82) Millefiori, S.; Favini, G.; Millefiori, A.; Grasso, D. *Spectrochim. Acta* **1977**, *33*, 21–27.
- (83) Flicker, W. M.; Mosher, O. A.; Kuppermann, A. *Chem. Phys. Lett.* **1977**, *45*, 492–497.
- (84) Kuppermann, A.; Flicker, W. M.; Mosher, O. A. *Chem. Rev.* **1979**, *79*, 77–90.
- (85) Walzl, K. N.; Koerting, C. F.; Kuppermann, A. *J. Chem. Phys.* **1987**, *87*, 3796–3803.
- (86) Pastore, M.; Angeli, C.; Cimiraglia, R. *Chem. Phys. Lett.* **2006**, *422*, 522–528.
- (87) Pastore, M.; Angeli, C.; Cimiraglia, R. *Chem. Phys. Lett.* **2006**, *426*, 445–451.
- (88) Angeli, C.; Pastore, M. *J. Chem. Phys.* **2011**, *134*, 184302.
- (89) Zdrozny, J. M.; Atanasov, M.; Bryan, A. M.; Lin, C.-Y.; Rekken, B. D.; Power, P. P.; Neese, F.; Long, J. R. *Chem. Sci.* **2013**, *4*, 125–138.
- (90) Nakao, Y.; Choe, Y.-K.; Nakayama, K.; Hirao, K. *Mol. Phys.* **2002**, *100*, 729–745.
- (91) Lu, Z.; Matsika, S. *J. Chem. Theory Comput.* **2012**, *8*, 509–517.
- (92) Gordon, M. S.; Schmidt, M. W.; Chaban, G. M.; Glaesemann, K. R.; Stevens, W. J.; Gonzalez, C. J. *Chem. Phys.* **1999**, *110*, 4199–4207.
- (93) Abrams, M. L.; Sherrill, C. D. *Chem. Phys. Lett.* **2004**, *395*, 227–232.
- (94) Kurlancheek, W.; Head-Gordon, M. *Mol. Phys.* **2009**, *107*, 1223–1232.
- (95) Karlström, G.; Lindh, R.; Malmqvist, P.-Å.; Roos, B. O.; Ryde, U.; Veryazov, V.; Widmark, P.-O.; Cossi, M.; Schimmelpfennig, B.; Neogrady, P.; Seijo, L. *Comput. Mater. Sci.* **2003**, *28*, 222–239.
- (96) McDiarmid, R. *Chem. Phys. Lett.* **1992**, *188*, 423–426.
- (97) Heimbros, L. A.; Kohler, B. E.; Levy, I. J. *J. Chem. Phys.* **1984**, *81*, 1592–1597.
- (98) Leopold, D. G.; Pendley, R. D.; Roebber, J. L.; Hemley, R. J.; Vaida, V. *J. Chem. Phys.* **1984**, *81*, 4218–4229.
- (99) Hudson, B. S.; Kohler, B. E.; Schulten, K. *Excited States*; Lim, E. C., Ed.; Academic: New York, 1982; Vol. 6, pp 1–95.
- (100) Cave, R. J.; Davidson, E. R. *J. Phys. Chem.* **1988**, *92*, 2173–2177.
- (101) D'Amico, K. L.; Manos, C.; Christensen, R. L. *J. Am. Chem. Soc.* **1980**, *102*, 1777–1782.
- (102) Bavia, M.; Bertinelli, F.; Taliani, C.; Zauli, C. *Mol. Phys.* **1976**, *31*, 479–489.
- (103) Tawada, Y.; Tsuneda, T.; Yanagisawa, S.; Yanai, T.; Hirao, K. *J. Chem. Phys.* **2004**, *120*, 8425–8433.
- (104) Watts, J. D.; Gwaltney, S. R.; Bartlett, R. J. *J. Chem. Phys.* **1996**, *105*, 6979–6988.
- (105) Lehtonen, O.; Sundholm, D.; Send, R.; Johansson, M. P. *J. Chem. Phys.* **2009**, *131*, 024301.
- (106) Kitao, O.; Nakatsuji, H. *Chem. Phys. Lett.* **1988**, *143*, 528–534.
- (107) Ostojić, B.; Domcke, W. *Chem. Phys.* **2001**, *269*, 1–10.
- (108) Weigend, F.; Häser, M.; Patzelt, H.; Ahlrichs, R. *Chem. Phys. Lett.* **1998**, *294*, 143–152.
- (109) Polli, D.; Altoe, P.; Weingart, O.; Spillane, K. M.; Manzoni, C.; Bida, D.; Tomasello, G.; Orlandi, G.; Kukura, P.; Mathies, R. A.; Garavelli, M.; Cerullo, G. *Nature* **2010**, *467*, 440–443.
- (110) Gozem, S.; Huntress, M.; Schapiro, I.; Lindh, R.; Granovsky, A. A.; Angeli, C.; Olivucci, M. *J. Chem. Theory Comput.* **2012**, *8*, 4069–4080.
- (111) Gozem, S.; Schapiro, I.; Ferré, N.; Olivucci, M. *Science* **2012**, *337*, 1225–1228.